Available online at www.sciencedirect.com
SCIENCE DIRECT®
Polymer 45 (2004) 2761–2771
polymer
www.elsevier.com/locate/polymer

Analysis of the non-linear viscoelastic behaviour of silica filled styrene butadiene rubber

C. Gauthier[a,*], E. Reynaud[a], R. Vassoille[a], L. Ladouce-Stelandre[b]

[a]GEMPPM umr 5510, INSA LYON, 20, av. A. Einstein F-69621 Villeurbanne Cedex, France
[b]C. R. A., Rhodia, 52 Rue de la Haie-coq, F-93308 Aubervilliers, France

Received 10 April 2003; received in revised form 11 December 2003; accepted 18 December 2003

Abstract

In the general background of the reinforcement of rubbers, the non-linear effect at small strains, generally referred as Payne effect, has been investigated in the case of silica-filled styrene–butadiene rubber (SBR). This work focuses on the influence of temperature, filler amount and surface treatment of silica particles. The experimental results demonstrate that the Payne effect occurs even at low silica content, below the percolation threshold. Moreover, the surface treatment appears to play a key role on the amplitude of the phenomenon. The use of coupling agents that promote covalent bounds between rubber and fillers reduces the amplitude of the non-linear phenomenon. At last, in order to describe the experimental data, a modelling approach is developed including (i) a mechanical model, based on self-consistent schemes, which could give account for the measured viscoelastic modulus given the complex composite microstructure and its evolution under stress (ii) a numerical description of the physical mechanisms associated with the Payne manifestation i.e. the debonding of the polymeric chains from the filler surface.

Keywords: Styrene–butadiene rubber; Payne effect; Filler

1. Introduction

The incorporation of small particle size fillers to cross-linked elastomer matrix results in substantially improved mechanical properties [1,2]. Nowadays, the use of silica particles, instead of carbon black, has proved to be of interest in the reinforcement of rubbers. Such filled rubbers are characterised by specific non-linear mechanical behaviours including high hysteresis, stress softening (Mullins effect) and strain dependent dynamic modulus effect (Payne effect) [3–5]. Experimental data reported in literature give evidence that many factors affect the thermo mechanical properties of filled rubbers, such as molecular structure of rubbers; the shape, size and filler contents; and the rubber/filler interactions. Besides the numerous experimental investigations, the various processes that have been invoked to explain filler reinforcement of elastomers have been reviewed [6,7]. They include molecular surface slippage or rearrangements, particle displacements, molecular segment alignment, inter particle chain breakage, strong and weak surface binding and other network particle surface phenomena. Most of these processes depend upon the nature of the interactions between the particle surface and the network molecular segments. Nevertheless there are still remaining questions about the mechanisms involved in the Payne effect. The aim of this work is to evaluate the Payne effect in a silica filled styrene butadiene rubber (SBR) in order to (i) evaluate the pertinent features of this non-linear effect, (ii) to analyse experimental data through the modelling of the strain dependant viscoelastic behaviour of the material.

2. Theoretical survey

The introduction of nanoscopic fillers, such as carbon blacks or silica particles, in a rubbery matrix strongly modify the viscoelastic behaviour of the material. In dynamic mechanical experiments, when submitted to successive sinusoidal deformation with increasing strain amplitude, the samples display a decrease of their storage modulus and the appearance of a maximum for the loss modulus at a deformation level around 0.1. The amplitude

* Corresponding author.

0032-3861/$ - see front matter © 2004 Published by Elsevier Ltd.
doi:10.1016/j.polymer.2003.12.081

variations of the storage and loss moduli, so-called Payne effect, are general to all filled elastomers. This non-linearity at low deformation (not revealed in pure elastomer) is equivalently demonstrated in classical shear-stress measurement [7]: the apparent modulus measured as the slope of the stress–strain curve decreases strongly when deformation is increased. The amplitude of the Payne effect is known to decrease when the strain rate of measurement decreases, the phenomenon quasi-vanishes at strain rate below 10^{-6}. An increase of temperature has the same influence since it strongly decreases the initial modulus and much less the terminal one [8].

The Payne effect has been the subject of numerous theories which can be more or less classified in two main types: (i) filler structure models, (ii) matrix–filler bonding and debonding models. The existence of two different pictures of this phenomenon is directly related to the nanoscopic size of the filler for which it is impossible to neglect either filler–filler interaction (with or without the involvement of the matrix), or the filler–matrix interaction.

In the filler structure models, the filler–filler interactions are considered as preponderant. Payne [3] believed that dependence of the moduli with strain is essentially determined by the agglomeration and de-agglomeration of the filler network. In the case of carbon black filled elastomers, above the percolation threshold, the presence of filler network can be evidenced by electrical conductivity measurements. The rigidity of this structure depends on the rigidity of the filler–filler bonds. It is assumed that this filler network is damaged by the application of a strain of sufficient magnitude that leads to the loss of rigidity. The agglomeration and de-agglomeration of the filler network, which is a dissipative phenomenon, is assumed to be at the origin of the peak of the loss modulus. Under this assumption, the strain dependencies of both the viscous and elastic moduli have been modelled by Kraus [9], assuming Van der Waals interactions between particles. However, this model does not predict the values of the high and low amplitude moduli, neither the influence of temperature. At large deformation, the difference between unfilled and filled rubber contains the contribution arising from the inclusion of rigid particles. The estimation of the modulus at high amplitude can be performed from the Guth equation [10]. For low filler concentration, the prediction of this equation is close to that of the Christensen and Low 3-phase model [11]. The concept of occluded rubber (rubber within the irregular contour of an aggregate and shielded from external forces) is often introduced in conjunction with the filler aggregation models [12,13]. Under increased applied stress, the entrapped matrix within the aggregates collapses and the dynamic properties depend on the amount of immobilised rubber. Gerspacher [14] used a different formalism to describe the process of rupture and reformation of contacts between aggregates. It is assumed a distribution of pair of aggregates in the material, from a linked state to a separate state. The alternance, during DMA measurements, of these states (linked-detached-linked) is responsible for energy dissipation.

Some experimental features are hardly interpreted by this first set of models, based on the mechanical response of a filler network. The occurrence of Payne effect for filler content well below the percolation threshold is not consistent with the filler structure models. Moreover, it has been reported that similar Payne amplitudes are observed in systems in which only the dispersion of the fillers is different [7].

The second set of models assumes that the matrix–filler interactions are responsible for the Payne effect [15]. These models are based on the idea of adsorbed polymer at the filler surface (bound rubber) that display a decreased molecular mobility and may act as supplementary cross-links in the material. Then, under the increase of strain, a mechanism of adhesion and de-adhesion of polymer chains at the filler interface is proposed. Two main types of experiments support the presence of bound rubber. First, several studies of RMN shows that an immobilised rubber phase is formed on filler particles, which thickness is below a few nanometers [16,17]. Second, from swelling experiment, it can also be concluded that fillers immobilise non-vulcanised rubber since they prevent migration of this bound rubber into a surrounding solvent. The main formulation for debonding of the polymeric chains from the filler surface has been proposed by Maier and Goritz [18]. As a result of the adsorption mechanism, the filler–matrix bonds are regarded as either stable bonds or unstable. Both types of bonds contribute to the elastic modulus, but only the unstable ones are likely to desorb under the application of strain or and temperature. However this formulation does not take into account the contribution to the modulus value arising from the inclusion of rigid particles and therefore leads to unrealistic values of the number of unstable bounds.

To conclude, the mechanisms of the Payne effect probably involves the filler structure and the adsorbed chain. The viscoelastic nature of the mechanical coupling of the filler to the matrix, particularly shown by the recovery experiments, strongly suggest the role of the filler elastomer structure in which filler–filler bonds are made via an adsorbed layer of polymer. However, it is still necessary to develop a formalism that describes the different aspects of the phenomenon. In order to develop such a modelling approach, we have investigate the behaviour of a silica–rubber system in order to enlighten the pertinent experimental features of the process.

3. Experimental part

3.1. Materials and techniques

The samples in this study are made of aggregates of silica particles in a styrene–butadiene matrix (SBR). The SBR

matrix is based on 25 ± 2% styrene −73 ± 4% butadiene, with a glass transition $T_g = -20$ °C (DSC measurements on a Perkin–Elmer DSC7 at 10°/min). The molecular mass of the copolymer is $M_w = 222 \times 10^3$ g/mol and the polydispersity index 1.75. The silica, provided by Rhodia, consists of aggregates of quasi-spherical particles fused together. These quasi-spherical particles display a diameter of about 13 nm and a surface area around 160 m^2/g. They form 'strengthened' aggregates with sizes around 40 nm. When incorporated in the rubber, these aggregates are further associated into agglomerates (characteristic sizes ranging from 0.1 to a few microns) which at normal loading form a network in which a part of the polymer can be entrapped.

All the samples were compounded and moulded by Rhodia. The sample preparation was made in a Brabender Mixer, using a rate of 80 rpm. After the rubber was premixed at 155 °C for 1 min, 2/3 of silica filler was incorporated into the rubber with the surface treatment (when added), the rest of silica was incorporated 1 min later and the mixing was continued until an equilibrium torque value was reached (total mixing time around 5 min). Finally, 2 mm thick films were obtained from the blends using a calander device. Samples were prepared with various amount of silica (ranging from 5 to 30 wt%) and, at a same filler loading (20%), with different surface treatments. Use was made of coupling agents that are bifunctional molecules able to react with both polymer matrix and the filler surface. The bis(3-triethoxysilyl propyl)tetrasulfide (TESPT), commonly abbreviated Si69 has been chosen, and compared with a second coupling agent (Dynasilan 3201). One may note that, even without coupling agent, interactions between polymer and silica are present, namely Van der Waals bounds between the hydroxyl groups at the silica surface and the double bound of the butadiene segments or the phenyl rings in the styrene segment. For comparison, silica filled rubber was also prepared with a covering agent (aliphatic chains, with a length comparable to that of Dynasilan 3201), avoiding, more or less, the interactions between silica and rubber. In all the cases, the surface treatment corresponds to 70% of covered surface. Table 1 lists the characteristics of the materials used in this study.

Table 1
Sample references

Sample	Surface treatment	Weight content of silica (phr)
A1	Dynasilan 3201	14
A2	Dynasilan 3201	27
A3	Dynasilan 3201	58
A4	Dynasilan 3201	76
A5 (SBR matrix)	–	0
A6	–	58
A7	Si69	58
A8	Covering agent (RP 83)	58

According to the complete recipe, the 58-phr sample is filled with 20 vol% of silica.

As already introduced, the surface developed by nanoscopic filler makes preponderant the matrix–filler and filler–filler interactions which are key parameters for the filler dispersion during the composite processing [19]. For this reason, all the interpretation of the non-linear behaviour of filled elastomers in studies that deal with a modification of these interactions via chemical treatment of the filler surface, or via the matrix chemistry, must be done taking into account a possible modification of the dispersion. In the case of the materials prepared for this study, it has been checked (by X-rays and light diffusion techniques) that the same level of dispersion is obtained for the different samples (at given filler content).

The viscoelastic behaviour of the samples was characterised at very low strains, through Dynamic Mechanical Analysis. Measurements were performed on an inverted torsion pendulum apparatus already described in literature [20]. This device works in a helium atmosphere, in the temperature range of 100–700 K and frequency range of 5×10^{-5} to 5 Hz. Specimens, 10 × 25 × 2 mm, cut from the compression-moulded sheets were tested. The storage (G') and loss (G'') parts of the dynamic shear modulus and so the internal friction tan $\phi(G''/G')$ were measured as a function of temperature (from 100 to 350 K), with a heating rate of 1°/min, and a frequency of 1 Hz.

The Payne effect is generally studied from low to intermediate strains and under dynamical solicitations. A Metravib viscoanalyser was used to measure the viscoelastic data with dynamic displacement in the range of a few up to 800 μm. The tests were performed on rectangular samples (25 × 10 × 2 mm^3) in shear at 5 Hz and at different temperatures (between 23 and 90 °C). Considering the sample dimensions, the strain amplitude for sinus deformation was limited to 0.2. The sample aspect ratio was chosen to ensure that the sample was subjected to simple shear.

3.2. Viscoelastic behaviour of the materials

The dynamic modulus of the samples was first investigated at low strain, in the linear domain. The evolution of the real part of the modulus (G') and the loss factor (tan ϕ) vs. temperature were obtained for the filled SBR with different amounts of silica (Fig. 1(a) and (b)). Spectra recorded for non-reinforced SBR is given for comparison. When the amount of filler increases, the modulus is increased over the investigated temperature range and the magnitude of the main relaxation, related to the glass transition of the polymer, decreased. The presence of the fillers produces a slight change in the shape of the main relaxation peak: it becomes more asymmetric when the filler content increases. In addition, it has been checked by DSC that no significant shift of T_g is observed whatever the filler content. As far as the influence of the surface treatment is

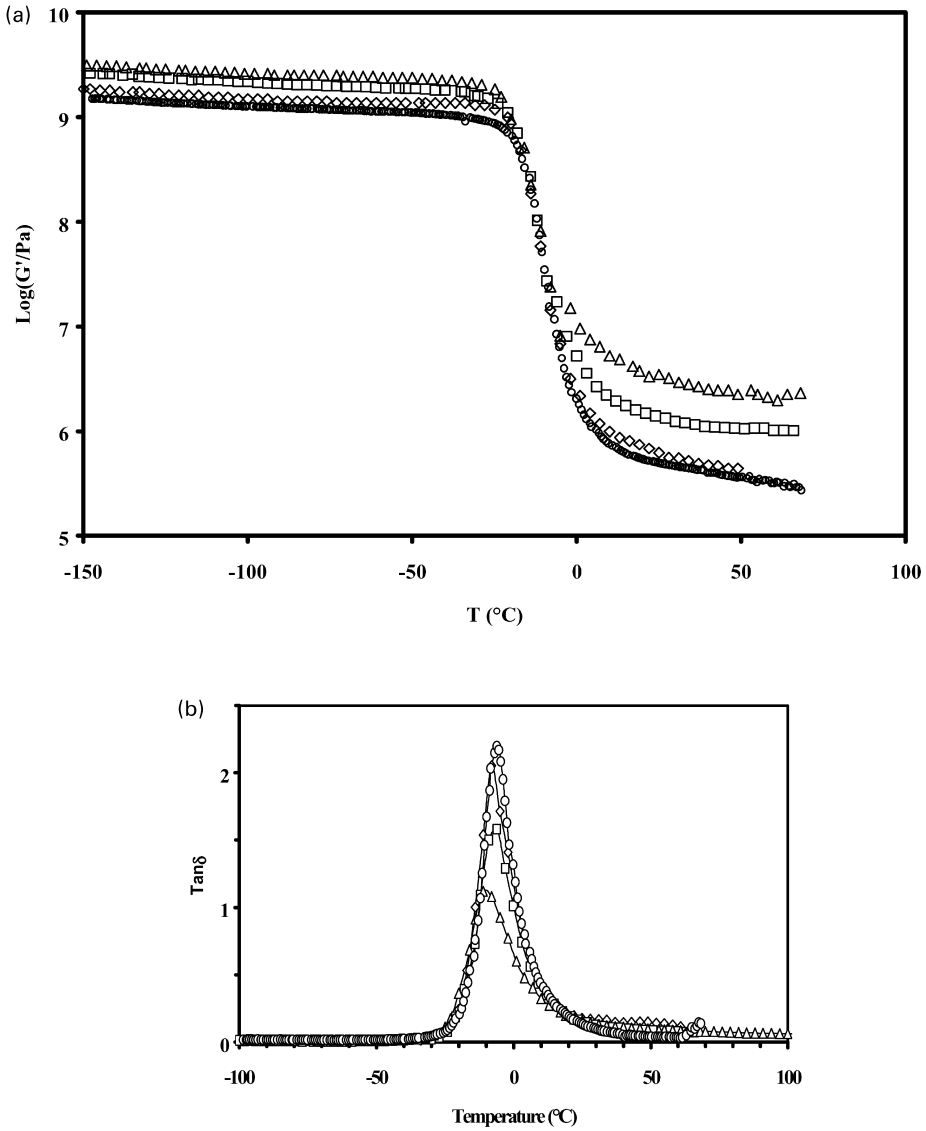

Fig. 1. (a) Storage modulus vs. temperature for filled elastomers with different silica volume fractions: (◇) A1, (□) A3, (△) A4, (○) A5. (b) Loss factor vs. temperature for filled elastomers for filled elastomers with different silica volume fractions: (△) A1, (□) A3, (◇) A4, (○) A5.

considered, differences are mainly observed in the values of the modulus in the rubbery plateau (Fig. 2(a) and (b)). The lowest values are obtained for the systems with chemical coupling agents (A3–A7), then with the covering agent (A8). The highest modulus in the rubbery plateau corresponds to the non-treated silica (A6).

3.3. Viscoelastic properties vs. strain

The viscoelastic behaviour vs. strain has been investigated and the results in Fig. 3 shows the typical qualitative features generally associated to Payne effect. The storage modulus is highest at small amplitude (hereafter referred to as G'_0) and monotonically decreases to a low value (hereafter G'_∞) (Fig. 3(a)). Note that the plateau at high dynamic amplitude is not reached, due to the strain limitation of the device. The loss modulus and loss factor curves show a typical loss peak, which occurs at approximately the same dynamic amplitude range where the storage modulus is most rapidly decreasing (Fig. 3(b)). In counterpart, it is found that the unfilled elastomer (A5) displays a linear viscoelastic behaviour, with no change in dynamic storage or loss modulus with strain amplitude in that investigated strain domain (the loss factor of A5 sample has a constant value of 0.3 on the whole amplitude range).

The influence of filler content, temperature and surface treatment can be further commented considering the evolution of the real part of the dynamic modulus (G') vs. strain. First, the magnitude of the Payne effect increases with increasing filler content (Fig. 3(a), Table 2). Actually, the non-linear effect is observed even at very low silica content, well below the percolation threshold. This point already invalidates the interpretation of the Payne effect based only on filler interactions. It can be noted that the

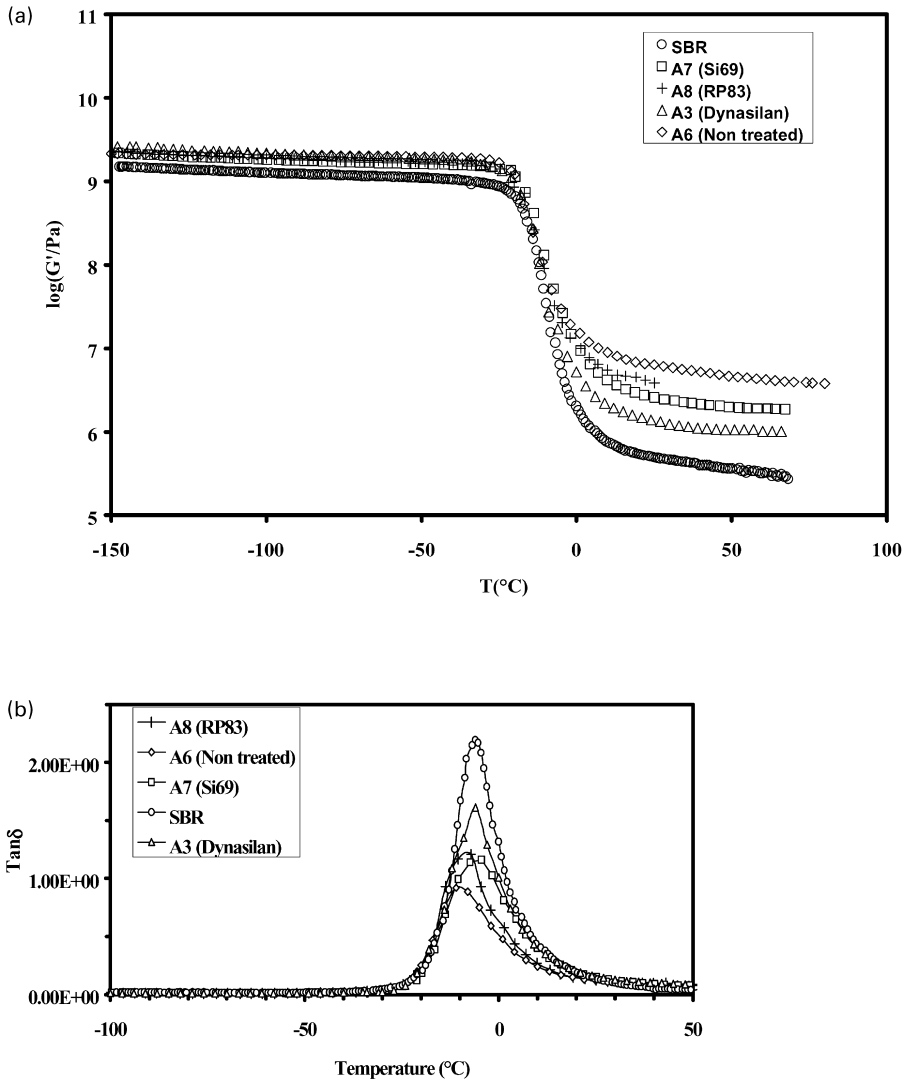

Fig. 2. (a) Storage modulus vs. temperature for filled elastomers with different surface treatments: (◇) A6, (□) A7, (+) A8, (△) A3, (○) A5. (b) Loss factor vs. temperature for filled elastomers with different surface treatments: (◇) A6, (□) A7, (+) A8, (△) A3, (○) A5.

values of the asymptotic modulus at low strain are in agreement with the measurements reported in Section 3.2 (taking into account the difference in frequency). At large deformation, the difference between unfilled and filled rubber ($G'\infty$) contains the contribution arising from the inclusion of rigid particles (generally accounted for by the Guth expression) and also the contribution of the polymer-filler cross-links to the network structure.

The influence of the temperature on the Payne behaviour has been investigated in the range from 23 to 90 °C, for the samples A3, A6 and A7. In all the cases, we observe a decrease of the magnitude of the non-linear effect when temperature increases: this decrease is mainly due to a decrease of the modulus at low strain (G'_0) while the high strain modulus ($G'\infty$) keep nearly the same value (Fig. 4 for sample A6, Fig. 9 for sample A7). As already observed by Payne, all the curves display the same shape when plotted in normalised way ($G' - G'\infty/G'_0 - G'\infty$ vs. strain). The decrease of the modulus at low strain has been previously reported to be an evidence for a thermally activated phenomenon [21]. It may be in relation with the constrained dynamics of the segmental motions of the rubber molecules interacting with the filler surface, as supported by NMR experiments [22,23].

At last, considering the influence of the surface treatment, at a same filler loading and similar surface area, we can observe that the surface treatment of silica with both coupling agents reduces drastically the magnitude of

Table 2
Amplitude of the Payne effect for SBR/silica samples with different filler contents

	G'_0 (MPa)	$G'\infty$ (MPa)	$\Delta G'$ (MPa)
A1	0.5	0.4	0.1
A2	0.85	0.7	0.15
A3	1.65	1.05	0.6
A4	2.8	1.6	1.2

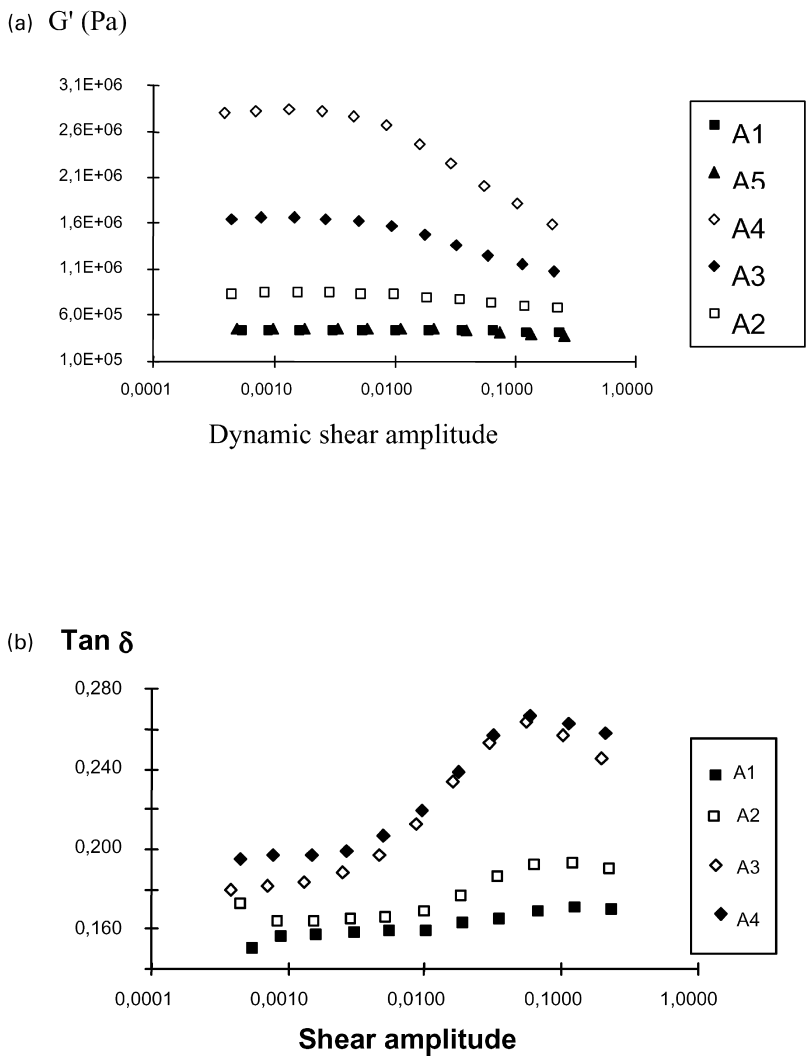

Fig. 3. (a) Storage modulus vs. dynamic amplitude for filled elastomers with different filler contents: (■) A1, (□) A2, (◆) A3, (◇) A4, (▲) A5. (b) Loss factor vs. dynamic amplitude for filled elastomers with different filler contents: (■) A1, (□) A2, (◇) A3, (◆) A4.

the non-linear effect (Fig. 5). The G'_0 values display more differences between both coupling system than the $G'\infty$ values. The non-linearity phenomenon amplitude is higher in the case of the covering agent (sample A8), but it is still smaller than the one observed for the untreated silica (sample A6). Actually, the untreated silica displays the highest decrease of modulus vs. strain that means the higher Payne effect. In view of these results, it appears that the presence of chemical bounds at the surface of silica, compared to untreated surface, weaken the interfacial

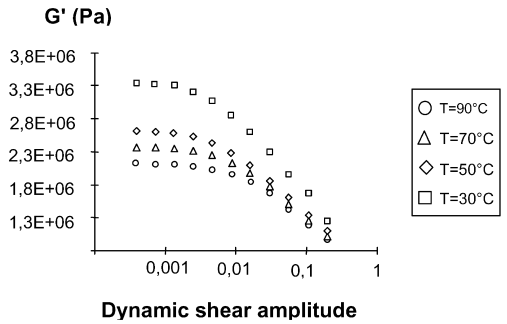

Fig. 4. Storage modulus vs. dynamic amplitude for 20% filled elastomer with non-treated surface (A6)-influence of temperature: (□) 30 °C, (◇) 50 °C, (△) 70 °C, (○) 90 °C.

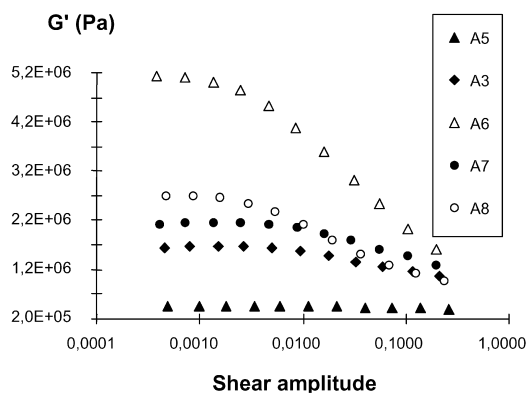

Fig. 5. Storage modulus vs. dynamic amplitude for filled elastomers with different surface treatments: (◆) A3, (▲) A5, (△) A6, (●) A7, (○) A8.

interactions between rubber and filler. If the Payne effect is attributed to a reduced segmental mobility of rubber molecules, it means that the chemical bounding causes less restricted mobility of macromolecules that might be difficult to understand. Considering the mechanism proposed by Maier and Goritz [18], it can be assumed that surface treatments by both coupling and recovery agent reduce the total number of physical temporary links and consequently reduces the Payne amplitude. In conclusion, our measurements evidence that the interfacial interactions play a key role in the amplitude of the Payne effect and the presence of chemical links at the silica surface limits the mechanisms accountable for this effect.

To conclude from our experimental data and the theoretical approaches found in literature, surface interactions between fillers and rubber molecules appear to be preponderant for the Payne effect: physical adsorption undoubtedly occurs to varying degrees depending on the particular surface. The softening mechanism may be due to dislocation of physical attachments; it may comprise displacement of physical cross-links to form longer network chains, together with re-attachments favouring the strained state of network chains.

4. Modeling part

Here comes out the need of putting these concepts into equations, so as to confront them to the experimental data. To sum it up, the milestone idea was that of the existence of bound rubber, related to the interactions between the filler surface and the polymer. As proposed by Maier and Goritz [18], a model of debonding of the polymeric chains from the filler surface may be used to describe the Payne effect. However, the chosen formulation has to include a mechanical description of the composite material. In that way, the theoretical approach to be developed has to involve:

- a numerical description of the evolution of the bound elastomer towards stress
- a mechanical model, which could give account for the measured viscoelastic data given the complex composite microstructure and its evolution under stress.

Bearing this in mind, a mechanical model is first proposed to account for the viscoelastic behaviour at small deformation. The three-phase model, first introduced by Christensen and Lo [13] was applied in three successive steps, as suggested by Shaterzadeh et al. [24]: this trick actually enables to account for both the existence of a rigid matrix phase near the filler-polymer interface (as determined from the model first step) and the influence of the silica structuration into aggregates (evaluated through the second step) onto the viscoelastic data of the composite as a whole.

Then, the same model is used to describe the Payne effect, taking into account the evolution of the filler/polymer interactions towards stress thanks to a thermo-mechanical activated process.

4.1. Mechanical coupling modelling of the linear viscoelastic behaviour

When a single uniform reinforcing phase is included in a uniform matrix, the 3-phase self-consistent model [13] is well suited for homogenisation of elastic randomly reinforced composites. It can be easily enlarged to linear viscoelasticity, assuming the Hashin correspondence principle [25] that substitutes complex module to the elastic ones. The $(n+1)$ phase model, proposed by Hervé and Zaoui [26], extends the 3-phase model to account for either true multi-layered inclusions or for property gradients at the inclusion-matrix interfaces. Thanks to the randomly spatial phase disposition, the morphology is only described by the volume fractions of the constituents anyway. Some difficulties arise with more complicated morphologies. The morphology itself must be statistically described before modelling the material properties [27]. Such approaches lead to complex theoretical models and involve very sophisticated tools to characterise the morphology.

When the composite contains aggregates, the morphology exhibits two or more scales of heterogeneity. The aggregates are a first composite at the lower scale whereas the real material is a composite of composites at the macroscopic scale. As an alternative to an increase of theoretical content, Christensen [28] generally suggested to estimate the effective properties of materials exhibiting several scales of heterogeneity by the n-step repetition of the 3-phase model. Franciosi and Gaertner [29] discussed extensively this approach in the context of polymer composites with a particular attention to the effects of interphases, modulus contrast and connectivity.

The morphology of filled rubbers can be schematically represented by Fig. 6 consists in a two-scale morphology exhibiting unreinforced zones and highly reinforced ones in which very close reinforcements are connected by a thin interphase of bound rubber (with lower mobility than the rest of the matrix). Then, thanks to the connectivity, we tried to describe such morphology by means of the 3-step repetition of the 3-phase model as schematically shown in Fig. 6. The first step gives the effective moduli of an equivalent resin i.e. both the bound rubber and the occluded rubber included in the concentrated composite. The bound rubber behaves then as a shell trapping the occluded rubber. After that, this equivalent resin is considered as the matrix surrounding the fillers in order to obtain the properties of the concentrated composite. In this second step, the highly reinforced zones are considered as a concentrated composite with a volume

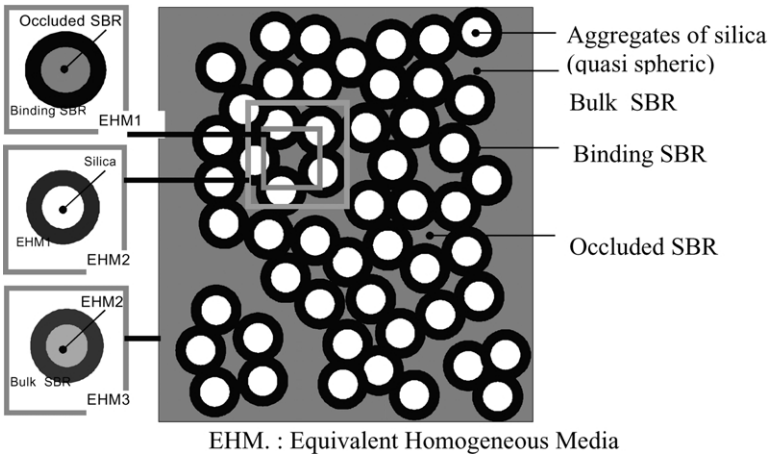

Fig. 6. Schematic description of filled rubber morphology and corresponding coupling model (self consistent 3-phase model applied in three successive steps).

fraction of reinforcement V_c greater than the nominal one V_n in the real composite. Lastly, in the third step, the 3-phase model is applied to obtain the effective moduli of the real composite by considering the highly reinforced zone included in the SBR matrix.

Calculations were performed as follows: the viscoelastic properties of occluded rubber and bulk matrix were experimental data for SBR, the glass was assumed to be elastic linear and its shear modulus is equal to 30 GPa all over the temperature range. The properties of the bound SBR was chosen equal to the properties of SBR in the glassy plateau (modulus around 1 GPa). The particle volume fraction in the aggregates was 35% for all the 20% filled rubbers, this allows to fit the modulus in the glassy plateau. Then, the fraction of the bound rubber, $v\ell$, is the only parameter to be fitted for each sample: $v\ell = 0.5\%$ for A3 and 6% for A6. The results of G' and $\tan(\phi)$ are shown in Fig. 7 in the case of A3 and A6 samples. The calculated and measured spectra are in very good agreement for the elastic and loss shear moduli, on the whole range of temperature.

4.2. Modelling of the Payne effect

Next, choice was made of describing the bound elastomer disruption as a thermo mechanically activated phenomenon. In other words, the equilibrium of the physical anchoring of the macromolecules onto the filler surface could be thermo mechanically displaced. With reference to a pseudo particle jump between two energetic wells, the evolution of the number of links between the filler and the surface could be statistically established as follows:

$$\Delta N = N_0 \frac{1 - \exp\left(\dfrac{\sigma v}{kT}\right)}{\left[1 + \exp\left(\dfrac{-\Delta U}{kT}\right)\right]\left[1 + \exp\left(\dfrac{\Delta U - \sigma v}{kT}\right)\right]}$$

where N_0 is the initial number of anchored polymer chains, ΔU is assimilated to an activation energy, and v represents the sensitivity towards desorption.

The model procedure was the following. The filler concentration within the aggregates and the volume of bound rubber at very low deformation was fixed by the

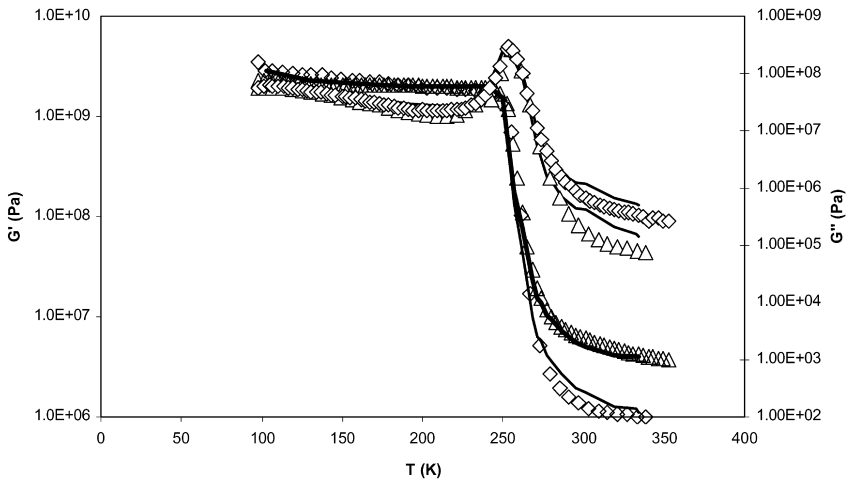

Fig. 7. Storage modulus and loss modulus vs. temperature for filled elastomers. Experimental data (◇) A3, (△) A6 and calculations (full line).

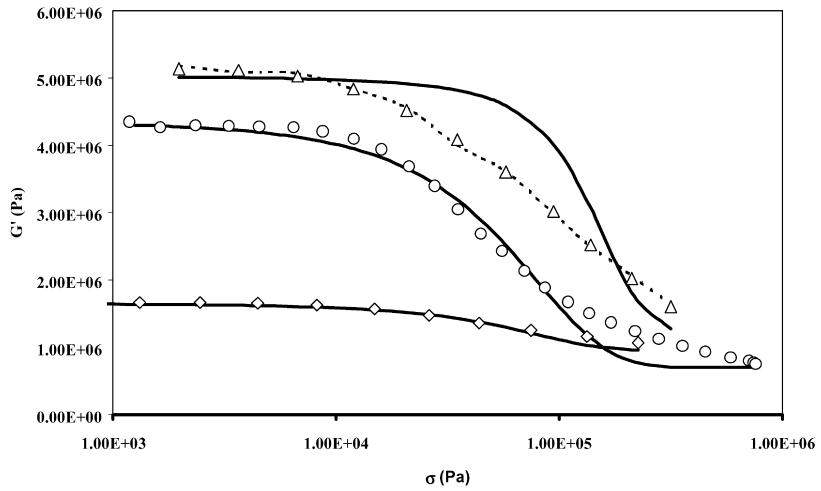

Fig. 8. Storage modulus vs. strain: experimental data and theoretical calculations (full lines) at $T = 23$ °C : (◇) A3, (△) A6 (○) A7.

viscoelastic modulus analysis ($G'(T)$). To relate the mechanical and statistical description, we assume that ΔN and $v\ell$ are proportional. The G'_∞ plateau corresponds to the case where no more bound rubber acts in the mechanical coupling within the composite. At a given temperature, an increase of stress or temperature leads to a decrease of ΔN i.e. of $v\ell$. The modulus is then recalculated, thanks to the 3-step repetition of the 3-phase model, taken into account the decrease of $v\ell$. The next step consists in optimising ΔU and ν values, so as to fit as best the experimental data corresponding to the Payne effect. Calculations were performed on three composite samples, namely A3, A6 and A7. (Fig. 8). Confrontation between experiments and theory was extended to various temperatures (full lines in Fig. 9). For any of the above experimental sets, the following parameters remain constant: the filler concentration within the aggregates was 0.35, ΔU reaches a value of 0.17 eV and ν was set equal to 1.5×10^{-25} Pa^{-1}. The evolution of the volume of anchored polymer vs. temperature turns out to follow an Arrhenius law, as shown in Fig. 10. When a single activation energy is used, we found that we can describe both plateau values but with the drop of modulus too straight. Hence, our calculations indicate the activation parameters may be distributed to obtain a better fit of the data. The influence of the distribution of the coefficient ν (with three ν values of respectively 1.5×10^{-25}, 5×10^{-25} and 10×10^{-25} Pa^{-1}) is illustrated in the case of the A6 sample (dot line on Fig. 8). This very simple distribution law enables to describe accurately the experimental data.

5. Conclusion

The aim of this study was to propose a theoretical description of the strain dependent non-linear effect in silica filled rubbers. Payne effect measurements were realized on silica filled SBR varying filler contant, temperature and surface treatment of silica. It was shown that the use of coupling agents that promote covalent bounds between rubber and fillers reduces the amplitude of the non-linear phenomenon. A modelling approach is developed including (i) a mechanical model, based on self consistent schemes, which could give account for the measured viscoelastic data given the complex composite microstructure and its evolution under stress (ii) a numerical description of the physical mechanisms associated with Payne manifestation i.e. the debonding of the polymeric chains from the filler

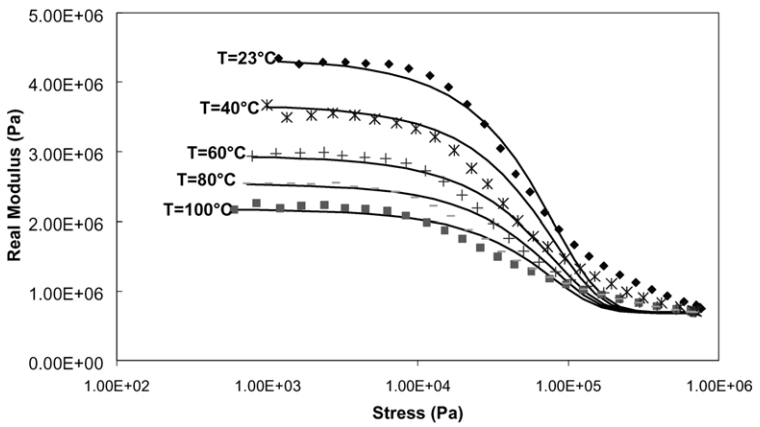

Fig. 9. Storage modulus vs. strain: experimental data and theoretical calculations (full lines) at various temperatures—case of A7 sample.

surface. This model allows reproducing the evolution of the modulus vs. temperature and vs. strain.

Appendix A. Appendix

The final solution from Herve and Zaoui for G^* of the particulate composite is given by the results of the quadratic Eq. (A1):

$$X\left(\frac{G_c^*}{G_m^*}\right)^2 + Y\left(\frac{G_c^*}{G_m^*}\right) + Z = 0 \tag{A1}$$

where, X, Y, and Z are constants. For three phase model, the following simplified expressions are:

$$\begin{aligned} X = {} & 4R_2^{10}(1-2\nu_m)(7-10\nu_m)H_{12} \\ & +20R_2^7(7-12\nu_m+8\nu_m^2)H_{42} \\ & +12R_2^5(1-2\nu_m)\times(H_{14}-7H_{23}) \\ & +20R_2^3(1-2\nu_m)^2H_{13} \\ & +16(4-5\nu_m)(1-2\nu_m)H_{43} \end{aligned} \tag{A2}$$

$$\begin{aligned} Y = {} & 3R_2^{10}(1-2\nu_m)(15\nu_m-7)H_{12} \\ & +60R_2^7(\nu_m-3)\nu_m H_{42} \\ & -24R_2^5(1-2\nu_m)\times(H_{14}-7H_{23}) \\ & -40R_2^3(1-2\nu_m)^2H_{13}-8(1-5\nu_m)(1-2\nu_m)H_{43} \end{aligned} \tag{A3}$$

$$\begin{aligned} Z = {} & -R_2^{10}(1-2\nu_m)(7+5\nu_m)H_{12}+10R_2^7(7 \\ & -\nu_m^2)H_{42}+12R_2^5(1-2\nu_m)\times(H_{14}-7H_{23}) \\ & +20R_2^3(1-2\nu_m)^2H_{13}-8(7-5\nu_m)(1-2\nu_m)H_{43} \end{aligned} \tag{A4}$$

which, $R_2 = 1$ and $H_{\eta\beta}$ are the products of the members of the following matrice P, thus $\eta(\beta)$ are the number of line (column) of the matrice H :

$$H_{12} = P_{1,1}\cdot P_{2,2} - P_{2,1}\cdot P_{1,2}$$
$$H_{13} = P_{1,1}\cdot P_{3,2} - P_{3,1}\cdot P_{1,2}$$
$$H_{14} = P_{1,1}\cdot P_{4,2} - P_{4,1}\cdot P_{1,2}$$
$$H_{23} = P_{2,1}\cdot P_{3,2} - P_{3,1}\cdot P_{2,2}$$
$$H_{42} = P_{4,1}\cdot P_{2,2} - P_{2,1}\cdot P_{4,2}$$
$$H_{43} = P_{4,1}\cdot P_{3,2} - P_{3,1}\cdot P_{4,2}$$

with matrix of P :

$$P = \frac{1}{5(1-\nu_m)}\begin{bmatrix} \frac{c}{3} & \frac{R_1^2(3b-7c)}{5(1-2\nu_f)} & \frac{-12\alpha}{R_1^5} & \frac{4(f-27\alpha)}{15(1-2\nu_f)R_1^3} \\ 0 & \frac{(1-2\nu_m)b}{7(1-2\nu_f)} & \frac{-20(1-2\nu_m)\alpha}{7R_1^7} & \frac{-12\alpha(1-2\nu_m)}{7(1-2\nu_f)R_1^5} \\ \frac{R_1^5\alpha}{2} & \frac{-R_1^7(2a+147\alpha)}{70(1-2\nu_f)} & \frac{d}{7} & \frac{R_1^2[105(1-\nu_m)+12\alpha(7-10\nu_m)-7e]}{35(1-2\nu_f)} \\ -\frac{5}{6}(1-2\nu_m)\alpha R_1^3 & \frac{7(1-2\nu_m)\alpha R_1^5}{2(1-2\nu_f)} & 0 & \frac{e(1-2\nu_m)}{3(1-2\nu_f)} \end{bmatrix}$$

with:

$$a = \left(\frac{G_f^*}{G_m^*}\right)(7+5\nu_f)(7-10\nu_m) - (7-10\nu_f)(7+5\nu_m)$$

$$b = 4(7-10\nu_f) + \left(\frac{G_f^*}{G_m^*}\right)(7+5\nu_f)$$

$$c = (7-5\nu_m) + 2\left(\frac{G_f^*}{G_m^*}\right)(4-5\nu_m)$$

$$d = (7+5\nu_m) + 4\left(\frac{G_f^*}{G_m^*}\right)(7-10\nu_m)$$

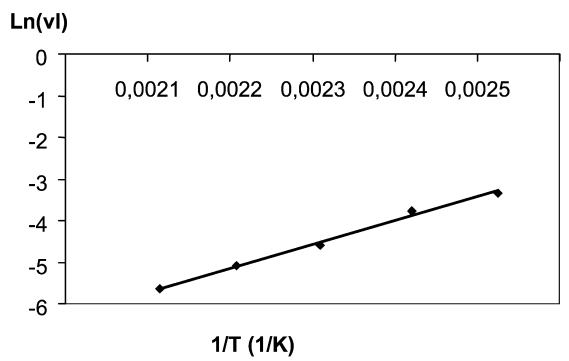

Fig. 10. Evolution of the volume fraction of anchored polymer within the composite vs. the temperature.

$$e = 2(4 - 5\nu_f) + \left(\frac{G_f^*}{G_m^*}\right)(7 - 5\nu_f)$$

$$f = (4 - 5\nu_f)(7 - 5\nu_m) - \left(\frac{G_f^*}{G_m^*}\right)(4 - 5\nu_m)(7 - 5\nu_f)$$

$$\alpha = \left(\frac{G_f^*}{G_m^*}\right) - 1$$

References

[1] Donnet JB, Riess G, Majowski G. Eur Polym J 1976;7:1065.
[2] Voet A. J Polym Sci, Macromol Rev 1980;15:327.
[3] Payne AR. J Appl Sci 1962;6(19):57–63.
[4] Payne AR, Whitaker RE. Rubber Chem Technol 1971;44:440.
[5] Harwood JAC, Mullins L, Payne R. J Appl Polym Sci 1965;9:3011.
[6] Wang MJ. Rubber Chem Technol 1998;71:520.
[7] Chazeau L, Brown JD, Yaniyo LC, Sterstein SS. Polym Compos 2000;21(no 2):202–22.
[8] Payne AR. Reinforcement of elastomers. New York: Interscience; 1965.
[9] Krauss G. J Appl Polym Sci, Appl Polym Symp 1984;39:75–92.
[10] Guth E. J Appl Mech 1945;16:20–5.
[11] Christensen RM, Lo KH. J Mech Phys Solids 1979;27:315–30.
[12] Medelia AI. J Colloid Interface Sci 1970;32:115.
[13] Medelia AI. Rubber Chem Technol 1973;46:877.
[14] Gerspacher M, O'Farrel CP, Yang HH, Tricot C. Rubber World 1996; 214:27.
[15] Funt JM. Rubber Chem Technol 1987;61:842.
[16] Asai S, Kaneki H, Sumita M, Miyasaka K. J Appl Polym Sci 1991; 43(7):1253.
[17] Vidal A, Haidar B. Elastomery 1999;3(4):28.
[18] Maier PG, Goritz D. Kautsch Gummi Kunsts 1996;49:18–21.
[19] Bréchet Y, Cavaillé J-Y, Chabert E, Chazeau L, Dendievel R, Flandin L, Gauthier C. Adv Engng Mat 2001;3:571.
[20] Cavaille JY, Salvia M, Merzeau P. Spectra 2000 1988;16:37–45.
[21] Lapra A. PhD Thesis, Université Pierre et Marie Curie, Paris IV, 1999.
[22] Polmanteer KE, Lentz W. Rubber Chem Technol 1975;48:795.
[23] Haidar B, Salah Derradgji H, Vidal A, Papirer E. Macromol Symp 1996;108:147.
[24] Shaterzadeh M, Gauthier C, Gerard JF, Mai C, Perez J. Polym Compos 1998;19(6):655–66.
[25] Hashin Z. Int J Solids Struct 1970;6:797–807.
[26] Hervé E, Zaoui A. Int J Engng Sci 1993;31(No. 1):1–10.
[27] Ponte Castaneda P, Willis JR. J Mech Phys Solids 1995;43(No. 12): 1919–51.
[28] Christensen RM. Mechanics of composite Materials. New York: Wiley/Interscience; 1979.
[29] Franciosi P, Gaertner R. Polym Compos 1998;19(1):81–95.